

Electronic Supplementary Information

NiMoO₄ nanorods with rich catalytic sites as superb electrocatalyst for cerium-based flow battery

*Xian XIE, Chung Yim CHAN, and Walid A. DAOUD**

* School of Energy and Environment, City University of Hong Kong, Tat Chee Avenue,

Kowloon, Hong Kong. E-mail: wdaoud@cityu.edu.hk; Tel: +852-3442-4499

Table S1. Comparison of all-vanadium, zinc-bromine and cerium-based RFB

RFB	Redox reactions	Theoretical cell voltage (V)	Current density (mA cm ⁻²)	Cost of electrolyte	
				Negative species (USD kg ⁻¹)	Positive species (USD kg ⁻¹)
All-vanadium	VO ₂ ⁺ + 2H ⁺ + e ⁻ ↔ VO ²⁺ + H ₂ O <i>E</i> ⁰ = 1.0 V	1.26	80-200	24	24
	V ³⁺ + e ⁻ ↔ V ²⁺ <i>E</i> ⁰ = -0.26 V				
Bromine-Zinc	Br ₂ + 2e ⁻ ↔ 2Br <i>E</i> ⁰ = 1.087 V	1.847	20-80	1.9	2.0
	Zn ²⁺ + 2e ⁻ ↔ Zn <i>E</i> ⁰ = -0.76 V				
Cerium-Zinc	Ce ⁴⁺ + e ⁻ ↔ Ce ³⁺ <i>E</i> ⁰ = 1.61 V	2.37	20-50	1.9	12
	Zn ²⁺ + 2e ⁻ ↔ Zn <i>E</i> ⁰ = -0.76 V				
Cerium-Vanadium	Ce ⁴⁺ + e ⁻ ↔ Ce ³⁺ <i>E</i> ⁰ = 1.61 V	1.87	50-100	24	12
	V ³⁺ + e ⁻ ↔ V ²⁺ <i>E</i> ⁰ = -0.26 V				

Table S2. Comparison of electrode modification approaches in all-vanadium RFB

Strategies	Approaches	Pros and cons
Introducing functional groups	Thermal treatment; Concentrated acid treatment; Electrochemical oxidation; Fenton's reagent treatment, etc.	Easy operation, limited performance, unsafe and not environmental friendly (for concentrated acid treatment)
Larger surface area	Nano-scaled carbon (graphene, graphene oxide, single/multi-walled carbon nanotubes) decorated GF; chemical etching, etc.	Boosting mass transfer; expensive (graphene: \$ 1/mg, platinum: \$ 0.0294/mg); roundabout and wasteful (for chemical etching)
Enhancing catalytic effect	Metal oxides deposition via hydrothermal reaction, impregnation, and electrochemical deposition, etc.	Show promising electrochemical performance, suffered from stability and scalability

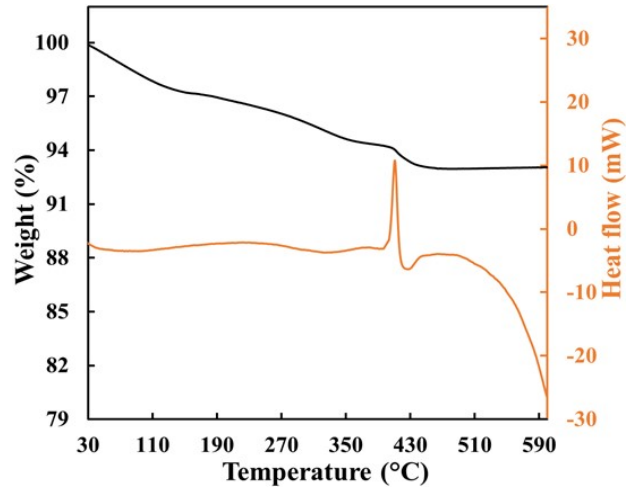


Fig. S1 TGA/DSC curve of $\text{NiMoO}_4 \cdot x\text{H}_2\text{O}$ precursor under N_2 environment

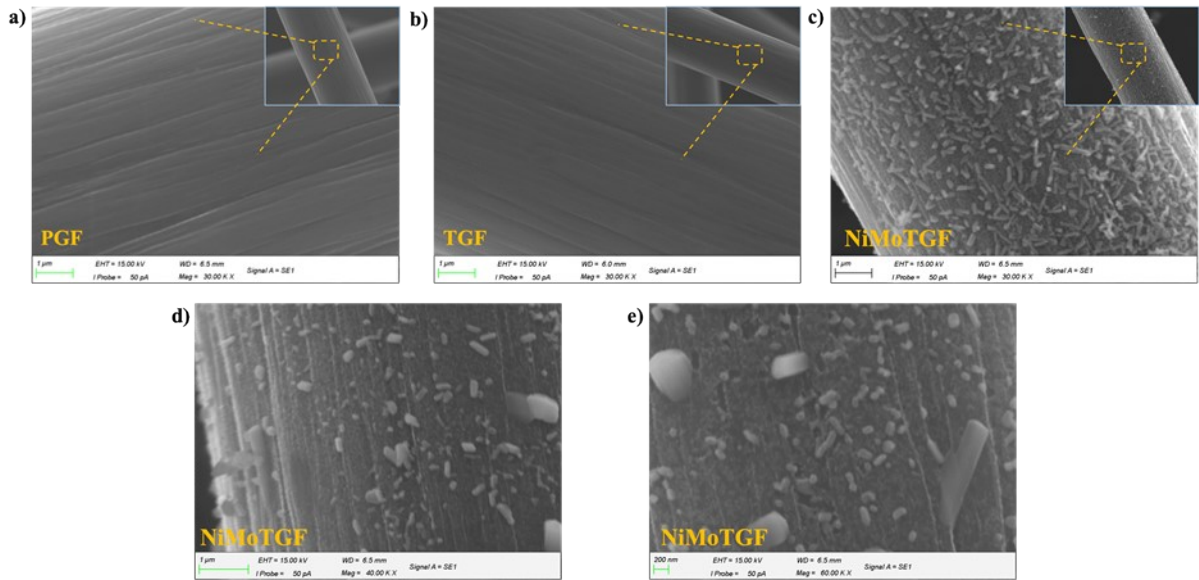


Fig. S2 SEM image of (a) PGF; (b) TGF at magnification of 30000; (c-e) NiMoTGF at magnification of 30000, 40000 and 60000, respectively

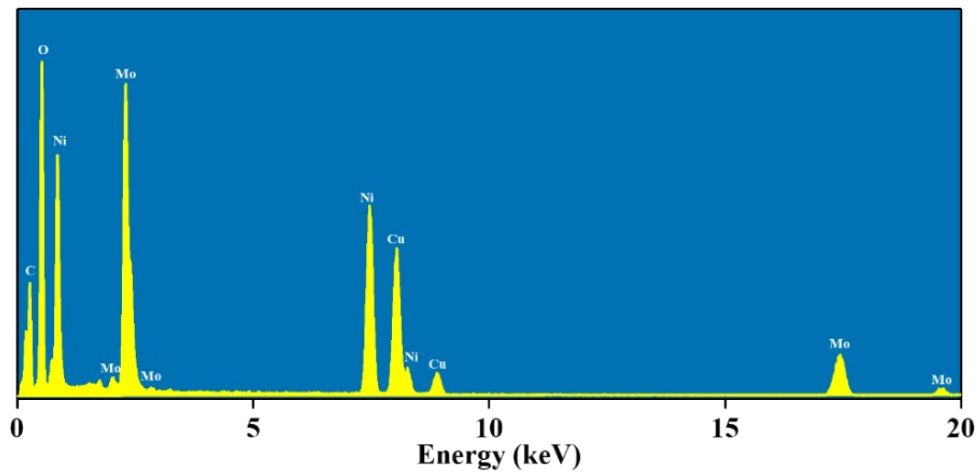


Fig. S3 HRTEM-EDS spectra of NiMoO_4 nanorod

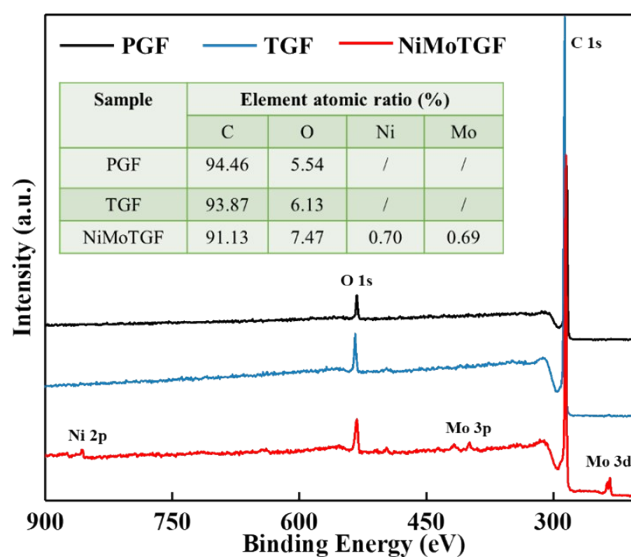


Fig. S4 XPS survey of PGF, TGF and NiMoTGF

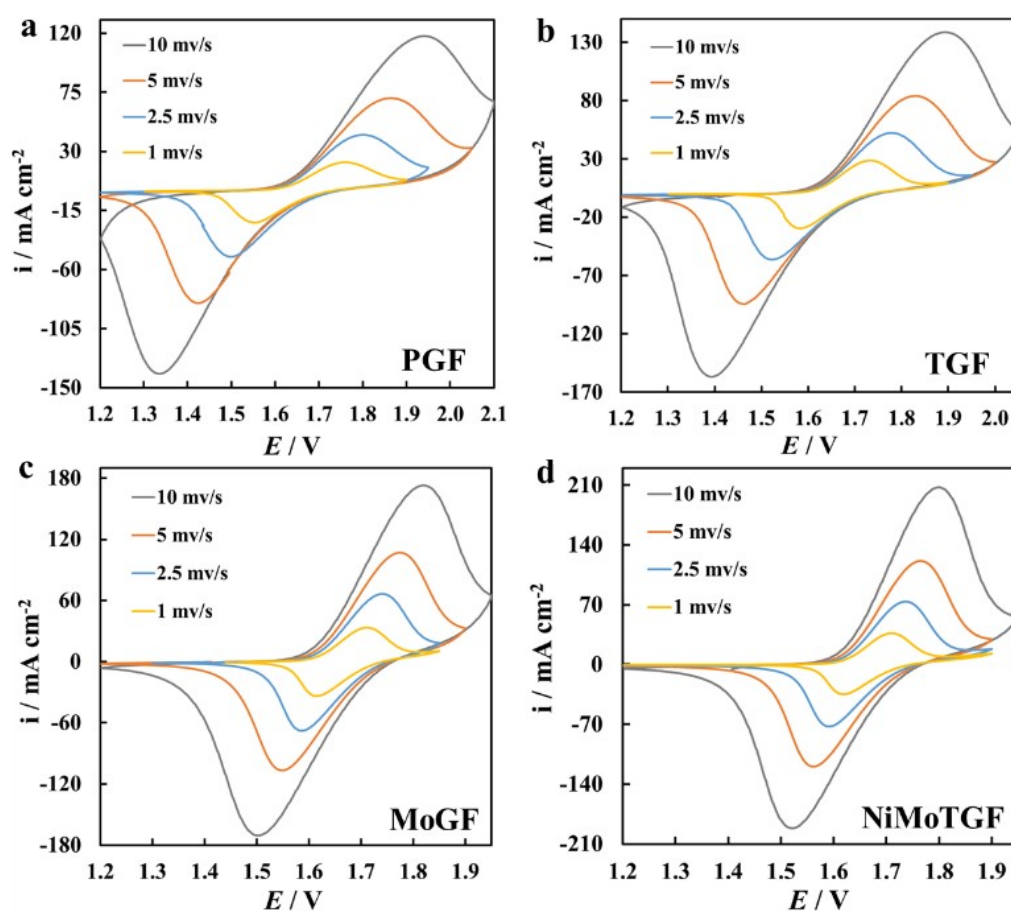


Fig. S5 CV profiles of (a) PGF; (b) TGF; (c) MoGF and (d) NiMoTGF at different scan rates

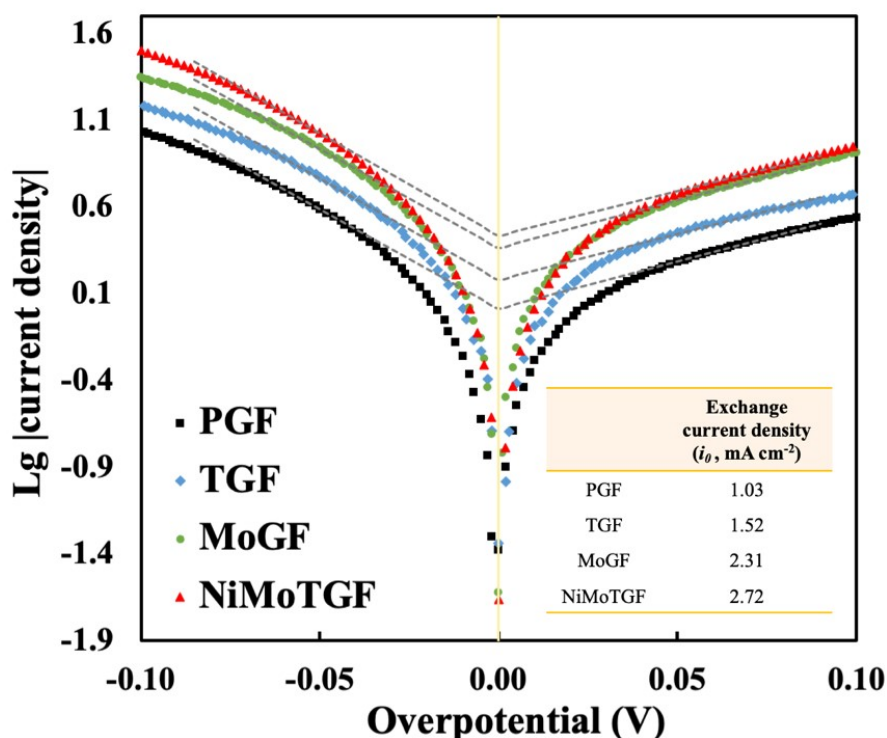


Fig. S6 Tafel plots of PGF, TGF, MoGF and NiMoTGF (derived from 1mv s⁻¹ CV profiles)

The kinetics of the Ce³⁺/Ce⁴⁺ reaction on graphite felt were analyzed using the Tafel equation:

$$\eta = \frac{2.3 RT}{\alpha n F} \lg i_0 \pm \frac{2.3 RT}{\alpha n F} \lg |i|$$

where i is the current density, i_0 is the exchange current density, α is the symmetry factor, n is the number of transferred electrons, F is the Faraday constant, R is the universal gas constant and T is the temperature. In particular, for a one-step single-electron-transfer reaction, the sum of α_c and α_a must equal unity, $\alpha_c + \alpha_a = 1$, where α_c and α_a are the cathodic and anodic transfer coefficient, respectively.¹ The linear Tafel fitting was performed and i_0 was calculated using the Tafel equation by knowing the intercept and Tafel slope.

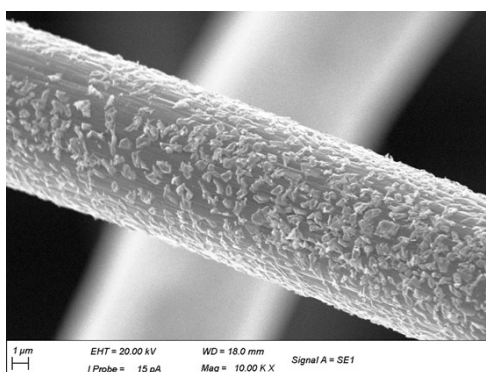


Fig. S7 SEM image of MoGF at magnification of 10000

Table S3. EIS fitting data acquired from EIS curves in **Fig. 7**

Sample	R_b (Ω)	CPE ₁		R_{ct} (Ω)	CPE ₂	
		V (F)	α		V (F)	α
PGF	0.52	0.78×10^{-3}	0.89	4.03	1.78	0.80
TGF	0.50	1.04×10^{-3}	0.89	1.83	1.39	0.76
NiMoTGF	0.48	1.23×10^{-3}	0.81	0.42	2.73	0.87

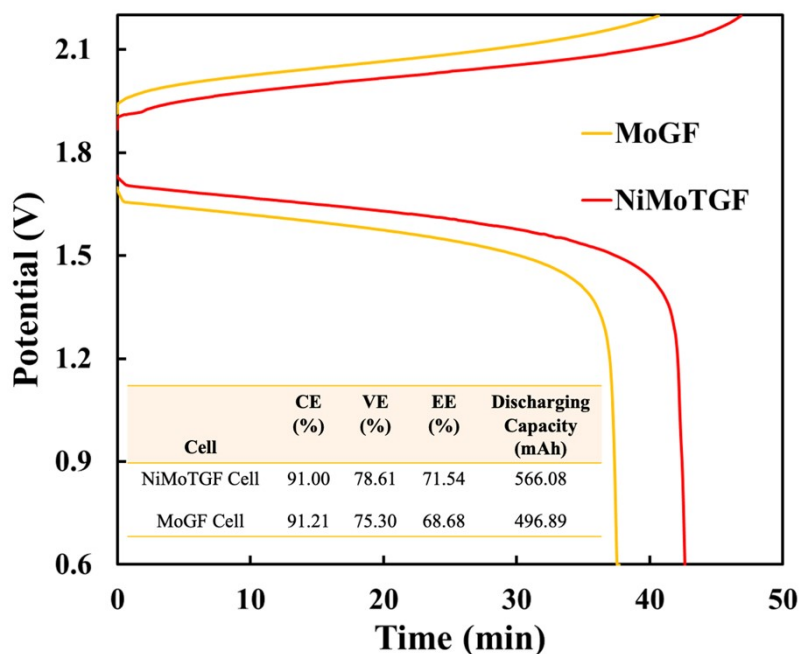


Fig. S8 Charge-discharge profiles and cell performance of MoGF and NiMoTGF cell

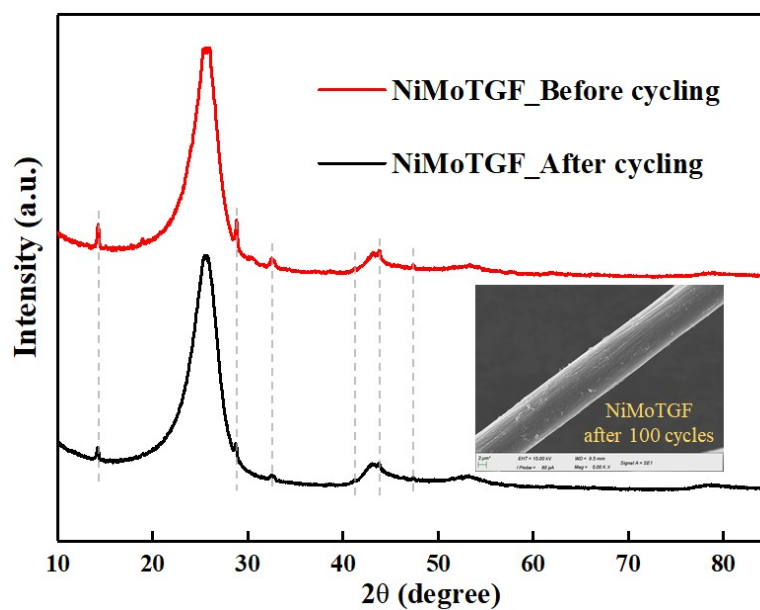


Fig. S9 XRD and SEM of NiMoTGF after 100 cycles

Table S4. Comparison of notable works on graphite felt electrode modification for cerium-based and all-vanadium flow batteries

Electrode material	Electrolyte (negative - positive)	Electrode preparation method	Membrane	Current density (mA cm ⁻²)	VE (%)	Discharging capacity increase (%) ^a	Ref.
Cerium-based flow battery							
SnO ₂	1.5 M Pb(II) - 0.5 M Ce(III), both in 1 M CH ₄ O ₃ S	Concentrated acid treatment, hydrothermal, calcination	GEFC-104	30 *	71.5	- (40 mAh fix capacity charging)	²
Metal-organic framework	1.5 M Pb(II) - 1 M Ce(III), both in 1 M CH ₄ O ₃ S	Impregnation, calcination, concentrated acid treatment	GEFC-104	30 *	68.5	- (40 mAh fix capacity charging)	³
All-vanadium flow battery							
Nitrogen-carbon nanospheres	0.75 M V(III) + 0.75 M V(IV) in 2 M H ₂ SO ₄ (both positive and negative electrolyte)	Polymerization, carbonization (900 °C, 2h)	Nafion 115	150 200 300 *	77 69.8 55.5	21.6 79.6 -	⁴
Reduced graphene oxide	0.75 M V(III) + 0.375 M V(IV) in 3 M H ₂ SO ₄ (both positive and negative electrolyte)	Chemical activation, hydrothermal	Nafion 115	150 200 300 *	81 74.5 63	285.5 - -	⁵
Surface exfoliation	1.5 M V(III) – 1.5 M V(IV), both in 3 M H ₂ SO ₄	Electrochemical exfoliation at 10 V	Nafion 115	150 200 *	74.4 61	63.5 32.13	⁶
Surface wrinkle	1.5 M V(III) – 1.5 M V(IV), both in 3 M H ₂ SO ₄	Hydrothermal, calcination	Nafion 115	150 200 300 *	78.5 72.5 59.8	33.3 - -	⁷
NiO	2 M V(III) - 2 M V(IV), both in 3 M H ₂ SO ₄	Impregnation, calcination	Nafion 117	125 150 *	77.5 72.5	62.2 -	⁸
NiCoO ₂	2 M V(III) - 2 M V(IV), both in 2.5 M H ₂ SO ₄	Hydrothermal, calcination	GN-114C	150 *	81.2	153.2	⁹
CeZrO ₂	2 M V(III) - 2 M V(IV), both in 2 M H ₂ SO ₄	Hydrothermal, calcination	Nafion 115	150 200 300 *	77.8 71.5 58.5	42.1 - -	¹⁰
MoO ₃	1.2 M V(III) – 1.2 M V(IV), both in 2.5 M H ₂ SO ₄	Impregnation, calcination	Nafion 117	150 200 250 *	81.0 76.1 71.4	139.7 - -	¹¹
ZrO ₂ metal-organic framework	0.8 M V(III) – 0.8 M V(IV), both in 3 M H ₂ SO ₄	Hydrothermal, calcination	Nafion 115	150 200 300 *	83 77.5 62.4	40 207 -	¹²
Cerium-vanadium flow battery							
NiMoO ₄	1 M V(III) in 5.5 M CH ₄ O ₃ S – 1 M Ce(III) in 3.5 M CH ₄ O ₃ S	Hydrothermal, calcination	Nafion 212	150 200 300 *	81.93 77.17 70.03	50.64 - -	This work

a. Discharging capacity increase over pristine graphite felt

* Highest current density reported

Reference

1. A. Heinritz, T. Binninger, A. Patru and T. J. Schmidt, *ACS Catal*, 2021, **11**, 8140-8154.
2. Z. Na, X. Wang, D. Yin and L. Wang, *J. Mater. Chem. A*, 2017, **5**, 5036-5043.
3. Z. Na, R. Yao, Q. Yan, X. Wang, G. Huang and X. Sun, *Energy Stor. Mater.* 2020, **32**, 11-19.
4. L. Wu, Y. Shen, L. Yu, J. Xi and X. Qiu, *Nano Energy*, 2016, **28**, 19-28.
5. Q. Deng, P. Huang, W.-X. Zhou, Q. Ma, N. Zhou, H. Xie, W. Ling, C.-J. Zhou, Y.-X. Yin, X.-W. Wu, X.-Y. Lu and Y.-G. Guo, *Adv. Energy Mater.* 2017, **7**.
6. A. Mukhopadhyay, Y. Yang, Y. Li, Y. Chen, H. Li, A. Natan, Y. Liu, D. Cao and H. Zhu, *Adv. Funct. Mater.* 2019, **29**, 1903192.
7. Z. Chen, Y. Gao, C. Zhang, X. Zeng and X. Wu, *Adv. Electron. Mater.* 2019, **5**.
8. N. Yun, J. J. Park, O. O. Park, K. B. Lee and J. H. Yang, *Electrochim. Acta*, 2018, **278**, 226-235.
9. Y. Xiang and W. A. Daoud, *J. Mater. Chem. A*, 2019, **7**, 5589-5600.
10. L. Yu, F. Lin, W. Xiao, L. Xu and J. Xi, *Chem. Eng. J.* 2019, **356**, 622-631.
11. X. Xie, Y. Xiang and W. A. Daoud, *ACS Appl. Energy Mater.* 2020, **3**, 10463-10476.
12. Y. Jiang, G. Cheng, Y. Li, Z. He, J. Zhu, W. Meng, L. Dai and L. Wang, *Chem. Eng. J.* 2021, **415**, 129014.